

AFCRL-57-0572

ATMOSPHERIC ABSORPTION OF SOLAR RADIATION
BY THE 9.6μ OZONE BAND

Aharon Goldman, David Murcray,
Frank Murcray, and Walter Williams

Department of Physics
University of Denver
Denver, Colorado

AD 661293

Contract AF 19(628)-5202
SCIENTIFIC REPORT NO. 6

Project No. 8662
Task No. 866201
Work Unit No. 86620101

NOV 17 1967

October 1967

This research was sponsored by the Advanced Research
Projects Agency Under ARPA Order No. 363

Contract Monitor: Charles V. Cunniff
Optical Physics Laboratory

Prepared for

Air Force Cambridge Research Laboratories
Office of Aerospace Research
United States Air Force
Bedford, Massachusetts

Distribution of this document is unlimited. It may be released to the
Clearinghouse, Department of Commerce, for sale to the general public.

AFCRL-67-0572

ATMOSPHERIC ABSORPTION OF SOLAR RADIATION
BY THE 9.6μ OZONE BAND

Aharon Goldman, David Murcray,
Frank Murcray, and Walter Williams

Department of Physics
University of Denver
Denver, Colorado

Contract AF 19(628)-5202

SCIENTIFIC REPORT NO. 6

Project No. 8662
Task No. 866201
Work Unit No. 86620101

October 1967

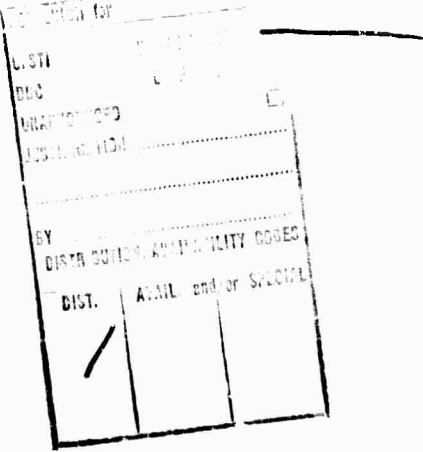
This research was sponsored by the Advanced Research
Projects Agency Under ARPA Order No. 363

Contract Monitor: Charles V. Curniff
Optical Physics Laboratory

Prepared for

Air Force Cambridge Research Laboratories
Office of Aerospace Research
United States Air Force
Bedford, Massachusetts

Distribution of this document is unlimited. It may be released to the
Clearinghouse, Department of Commerce, for sale to the general public.



Qualified requestors may obtain additional copies from the Defense Documentation Center. All others should apply to the Clearinghouse for Federal Scientific and Technical Information.

TABLE OF CONTENTS

	<u>Page</u>
ABSTRACT	vii
1. INTRODUCTION	1
2. THEORETICAL	3
2. 1. Statistical Model Method	3
2. 2. Line by Line Methods	5
3. RESULTS	7
4. CONCLUSIONS	10
ACKNOWLEDGMENTS	11
REFERENCES	12

LIST OF FIGURES

<u>Figure No.</u>	<u>Page</u>
1 Samples of the unreduced data showing the variation of the R-branch of the $9.6\mu\text{O}_3$ band with altitude. Each is labelled by record number (5 to 61) for which details are given in Table 1	13
2 The selected analytical density distribution used here for ozone, with the parameters $W = 0.218 \text{ cm-atm}$, $y_p = 25.0 \text{ km}$ and $h = 4.63 \text{ km}$	14
3 Comparison of observed and calculated transmittance by the $9.6\mu\text{O}_3$ band. The calculations were made using the statistical model combined with Curtis-Godson approximation with no water vapor present. The spectra are labelled according to record numbers, the details of each record number being given in Table 1. The relatively smooth curve is that of the reduced data while the wiggly curve is the theoretical curve	15
4 Comparison of transmittance obtained by exact line by line calculation, curve (1); by the combination of Curtis-Godson approximation and line by line calculation, curve (2); and by the combination of Curtis-Godson approximation and the statistical model curve (3); for the $9.6\mu\text{O}_3$ band. All the curves are calculated for Rec. 9 using the ozone distribution described in Fig. 2. Details for Record 9 are given in Table 1. The two upper curves are displaced by 20%	17
5 Comparison of transmittance obtained by exact line by line calculation, curve (1); by the combination of Curtis-Godson approximation and line by line calculation, curve (2); and by the combination of Curtis-Godson approximation and the statistical model, curve (3); for the $9.6\mu\text{O}_3$ band. All the curves are calculated for Rec. 20 using the ozone distribution described in Fig. 2. Details for Rec. 20 are given in Table 1. The two upper curves are displaced by 20%	18

LIST OF FIGURES (Cont.)

Figure No. Page

6 Comparison of transmittance obtained by exact line by line calculation, curve (1); by the combination of Curtis-Godson approximation and line by line calculation, curve (2); and by the combination of Curtis-Godson approximation and the statistical model, curve (3); for the $9.6\mu\text{O}_3$ band. All the curves are calculated for Rec. 61 using the ozone distribution described in Fig. 2. Details for Rec. 61 are given in Table 1. The two upper curves are displaced by 20% 19

ABSTRACT

The statistical band model, combined with the Curtis-Godson approximation is applied to the analysis of atmospheric slant path absorption of the $9.6\mu\text{ O}_3$ band. The theoretical spectra are compared with experimental absorptions observed during a balloon flight during which spectra were obtained at altitudes up to 30 km. The results are shown to agree to within the accuracy of the data. The band model method of calculation is compared to exact line by line calculation and to the combination of the Curtis-Godson approximation and line by line calculation. A surprisingly close agreement is found between the different methods of calculation, confirming the success of the application of the band model method to the data.

1. INTRODUCTION

Two balloon flights were made during the fall of 1966 during which the variation of the infrared solar spectrum with altitude in the 9.6μ region was observed. The instrumentation used to obtain the data has been described in detail in a recent paper.¹ Some of the data obtained during these flights and an analysis of the $9.6\mu O_3$ absorptions observed are presented in this study.

As an example of the data obtained, the variation of the R-Branch of the $9.6\mu O_3$ band with altitude is shown in Fig. 1. The resolution is estimated to be about 0.8 cm^{-1} . The structure seen is a combination of the absorption and the noise which are unfortunately of similar magnitude. Certain absorption lines at the lower altitudes are the result of contributions due to H_2O and CO_2 superimposed on the O_3 lines. The most significant of these in the region covered by Fig. 1 are at 1074.50 cm^{-1} and 1066.20 cm^{-1} . These have been identified in solar spectra taken from the ground.² Each of these absorptions embraces several lines due to the ν_2 and the $\nu_3 - 2\nu_2^0$ bands of H_2O and CO_2 , respectively:

1074.50 cm^{-1} : $9_{-3} - 10_{-6}, 4_{-4} - 5_4$ due to $\nu_2 H_2O$ and

$R16, R14, R12$ due to $\nu_3 - 2\nu_2^0 CO_2$

1066.20 cm^{-1} : $9_{-9} - 10_{-5}, 6_0 - 7_4$ due to $\nu_2 H_2O$ and

$R0, R2, R4$ due to $\nu_3 - 2\nu_2^0 CO_2$

In the P-Branch, not seen in Fig. 1, a few rotational lines due to H_2O are also present. It is seen from Fig. 1 that above 10 km the contributions of H_2O and CO_2 are no longer significant. Thus for all records obtained above 10 km a pure ozone analysis may be considered, with no H_2O or CO_2 present.

It should be noted that ozone is a difficult gas to handle quantitatively in the laboratory and has also been difficult to treat theoretically. As a result it is only recently that individual line parameters have become available, and these are still in some doubt.³ In view of this the prediction of the absorption by using accurate line by line calculation is also in some doubt.

In general any analysis of the slant path experimental spectra is complicated by the fact that for an atmospheric path along which there

is a variation of pressure, the absorption line is no longer a Lorentz line. Calculation of the exact spectrum requires then the integration over the exact line shape. This integration may be eliminated by the use of the Curtis-Godson (or CG) approximation which uses an equivalent Lorentz line. The exact line by line calculation may also be approximated by incorporation of the CG approximation into a band model thus providing a simple way for calculating spectra.

It should be noted that at high altitudes the line shape changes from Lorentz shape, through Voigt shape, to Doppler shape. While the Lorentz half-width is equal to the Doppler half-width at about 31 km the contribution of the Doppler case to the transmittance becomes significant only at considerably greater heights.⁴ In view of the fact that for the ozone distribution used here only a few percent of the total ozone amount is above 40 km, only the Lorentz line is used in this analysis.

In earlier studies the CG approximation combined with a band model was applied successfully to many infrared bands.⁴ However it was concluded in the past that the statistical band model does not fit the $9.6\mu \text{ O}_3$ band and, further, that the Curtis-Godson approximation is inadequate for atmospheric ozone calculations.⁴ In recent studies it was demonstrated, both theoretically³ and experimentally,⁵ that the statistical model does fit the $9.6\mu \text{ O}_3$ band. Since the band model expressions can be applied only to homogeneous paths at constant temperature and pressure, the real atmospheric ozone path must be reduced to an equivalent path at constant temperature and pressure. This suggested the approach of the present work which uses a combination of the statistical model and the Curtis-Godson approximation.

It is shown that the combination band model - CG is a good approximation to a precise line by line calculation over the ozone distribution and also to the combination of a line by line calculation and the Curtis-Godson approximation. It should be noted that the comparison made here between the combination statistical model - CG approximation and the combination line by line - CG approximation is equivalent to the comparison made previously³ between the statistical model and the line by line calculation for homogeneous path. It is found that the agreement among the above three methods is surprisingly close, explaining why the application of the statistical model to the balloon flight data gives satisfactory results.

Section 2 gives a description of the band model procedure followed by the description of line by line procedures. In Section 3 the band model procedure is applied to the flight data and compared with the line by line calculations. Conclusions are reached in Section 4.

2. THEORETICAL

2.1. Statistical Model Method

This procedure combines the statistical band model and the Curtis-Godson approximation. A "standard" ozone vertical distribution $\rho(y)$ is assumed

$$\rho(y) = \frac{W \exp((y-y_p)/h)}{h[1 + \exp((y-y_p)/h)]^2}, \quad (1)$$

with three parameters, W , y_p and h . Here y is taken as a vertical coordinate measured upwards from the ground (in km). This function was previously used by Green⁶ with the parameters

$$W = 0.218 \text{ cm-atm} \quad y_p = 23.25 \text{ km} \quad h = 4.53 \text{ km}, \quad (1A)$$

chosen to fit a "standard" ozone distribution proposed by Altshuler.⁷ These three parameters determine, respectively, the total amount of ozone, the height of the peak of the distribution, and the width of the distribution.

From the above distribution an equivalent pressure p_E (in atm) is calculated for a record taken at altitude y_0 and zenith angle θ according to

$$p_E = p_E(y_0) = \frac{\int_{y_0}^{\infty} p(y)\rho(y)dy}{\int_{y_0}^{\infty} \rho(y)dy} = \frac{\int_{y_0}^{\infty} p(y)\rho(y)dy}{W[1 + \exp((y-y_p)/h)]^{-1}}, \quad (2)$$

where $p(y)$ is the atmospheric pressure (in atm).

This calculation of p_E is equivalent to Curtis-Godson approximation. The atmospheric pressure is taken from U. S. Standard Atmosphere, 1962,⁸ and the integration of $p(y)\rho(y)$ is performed numerically. For somewhat greater accuracy in this calculation, one might use in place of $p(y)$ the effective broadening pressure p_e , given by

$$p_e(y) = p_t(y) + (B-1) p_a(y)$$

Here B is the self-broadening coefficient of the absorbing gas, $p_a(y)$ is the partial pressure of the absorbing gas and $p_t(y)$ is the total pressure of the gas mixture. Estimate of B is reported by Walshaw⁹ as 1.61. In view of the small partial pressure of ozone in the atmosphere, (partial pressure up to 200 μmb), a good approximation is made by assuming $p_e(y) \approx p(y)$. In addition to p_E , an equivalent pathlength L_E is calculated from (1) according to

$$\begin{aligned} L_E &= L_E(y_0, \sec\theta) = \frac{\left(\int_{y_0}^{\infty} \rho(y) dy \right) \sec\theta}{p_E(y_0)} \\ &= \frac{W \sec\theta}{[1 + \exp((y - y_p)/h)] p_E(y_0)} \end{aligned} \quad (3)$$

In this expression L_E contains the $\sec\theta$ factor while p_E is independent of the zenith angle.

It would be desirable to construct curves of growth by plotting $\frac{-\ln \bar{T}}{p_E}$ vs L_E , where \bar{T} is the measured transmittance averaged over a wide enough slit, and thus obtain the band model parameters¹⁰ from the flight data. However, it is found in the following that the range of L_E throughout the flight records is quite small and this precludes the use of this way of treating the data. A different method is therefore needed for obtaining these parameters.

The statistical band model parameters $(x/L_E)_v$ and $(2\pi\gamma^0/d)_v$, can be calculated from quantum mechanical data for individual line parameters according to³

$$\left(\frac{x}{L_E} \right)_v = \frac{1}{8} \frac{(\sum_i S_i^0)^2}{\left(\sum_i S_i^{0 \frac{1}{2}} \gamma_i^{0 \frac{1}{2}} \right)^2} \quad (4A)$$

$$\left(\frac{2\pi \gamma^0}{d} \right)_v = \frac{8}{\Delta v} \frac{\left(\sum_i S_i^{0 \frac{1}{2}} \gamma_i^{0 \frac{1}{2}} \right)^2}{\sum_i S_i^0} \quad (4B)$$

Here x is defined as $S^0 p_a L / 2\pi\gamma$, where S^0 is the integrated intensity of a line ($\text{cm}^{-2} \text{atm}^{-1}$), p_a is the partial pressure of the absorbing gas (atm), L is the optical path, γ is the half-width of a line (cm^{-1}), γ^0 is the half-width per unit pressure ($\text{cm}^{-1} \text{atm}^{-1}$), and d is the average spacing between lines (cm^{-1}). The sums are taken over all spectral lines in the interval $\Delta v (\text{cm}^{-1})$ for the center of which the parameters are calculated.

The average transmittance \bar{T}_v is then calculated for each record with the two slant path parameters, L_E and p_E , according to³

$$\bar{T}_v = \exp \left[- \left(\frac{2\pi \gamma^0}{d} \right)_v p_E \frac{(x/L_E)_v L_E}{\sqrt{1+2\left(\frac{x}{L_E} \right)_v L_E}} \right]. \quad (5)$$

In the above analysis there are only a few parameters to be fitted for best agreement with the experimental data: W , y_p , h , the ozone distribution parameters; T , the temperature; γ^0 , the half-width and S^0 , the intensity.

2.2. Line by Line Methods

A comparison is given herein of the above analysis with an accurate line by line calculation over the ozone distribution. The monochromatic transmittance T_v of an atmospheric slant path from the pressure level $p = p_0$, at altitude y_0 , to the top of the atmosphere, $p = 0$ is

$$T_v = \exp \left(- \int_{p_0}^0 k_v du \right), \quad (6)$$

where k_ν is the absorption coefficient and u is the optical mass. The integration with respect to u is for a path along which both the half-widths and the line intensities may vary. It is assumed here that the path is isothermal, so that no temperature variation along the path is considered. The exact calculation for a Lorentz line spectrum is given then by

$$T_\nu = \exp \left[-\frac{\sec \theta}{\pi} \sum_{i=1}^N S_i^0 \int_{y_0}^{\infty} \frac{p(y) \gamma_i^0 p(y) dy}{(\nu - \nu_{0i})^2 + p(y) \gamma_i^0} \right], \quad (7)$$

where ν_{0i} are the line centers (cm^{-1}) and the summation is over all N lines which contribute to the absorption at frequency ν . The line intensities S_i^0 are assumed to depend on temperature T ($^\circ\text{K}$) according to

$$S^0(T) = S^0(T_0) (T_0/T)^{3/2} \exp \left(-1.439 E'' \left(\frac{1}{T} - \frac{1}{T_0} \right) \right), \quad (8)$$

where E'' (cm^{-1}) is the lower state energy. Here a $(T_0/T)^{3/2}$ temperature dependence of the partition function for asymmetric top molecules is assumed.

The transmittance is then degraded by a slit function $g(\nu - \nu')$, $2a(\text{cm}^{-1})$ wide, according to

$$\bar{T}_\nu = \frac{\int_{\nu-a}^{\nu+a} g(\nu - \nu') T_{\nu'} d\nu'}{\int_{\nu-a}^{\nu+a} g(\nu - \nu') d\nu'} \quad (9)$$

where $T_{\nu'}$ is the monochromatic transmittance as given by equation (7) and ν is the center of the interval of calculation.

A comparison is also given herein of the present analysis with the combination of CG approximation and line by line calculation. The manner in which the CG approximation is used here is by calculating an equivalent half-width $\bar{\gamma}$ according to

$$\bar{\gamma}_i = \gamma_i^0 P_E \quad (10)$$

where p_E is given by equation (2). The monochromatic transmittance, then, is calculated by

$$T_\nu = \exp \left[-\frac{\sec \theta}{\pi} \left(\int_{y_0}^{\infty} \rho(y) dy \right) \sum_{i=1}^N \frac{s_i^0 \bar{\gamma}_i}{(\nu - \nu_{0i})^2 + \bar{\gamma}_i^2} \right] \quad (11)$$

Here $\sec \theta \left(\int_{y_0}^{\infty} \rho(y) dy \right)$ is the amount of ozone in the slant path above y_0 .

Equation (11) is similar to equation (7) except that the integration over the ozone distribution for each line is eliminated, thus greatly simplifying the numerical calculation. The transmittance is then degraded by a slit function using equation (9).

In the following calculations a square slit function was used, with $2a = \Delta\nu$, corresponding to the band model calculation.³ The integrated absorption A is given by

$$A = \int_{\nu_1}^{\nu_2} A_\nu d\nu = \int_{\nu_1}^{\nu_2} (1 - T_\nu) d\nu , \quad (12)$$

where ν_1 and ν_2 are the frequency limits of the band. The expression A is independent of the spectral slit width.

Equations (7), (9), (11) require elaborate numerical calculations for which large, high speed computers are needed.

3. RESULTS

The balloon flight data were reduced using a straight line envelope drawn by inspection, relying mainly on the short wavelength branch of the data. The zero level was determined from broad seeker "absorptions" and the calculated transmittance was then numerically degraded by a square filter equivalent to 2.5 cm^{-1} . The 2.5 cm^{-1} interval was chosen because it was previously found³ that it is wide enough for the statistical model to be applicable for the 9.6μ band.

The theoretical computations were made using equations (7)-(9) for the exact line by line calculations, equations (10), (11), (9) for the

combined CG-line by line calculations and equations (2)-(5) for the combined CG-statistical model calculations.

The statistical model method combined with CG approximation was applied to records above 10 km, assuming no H₂O or CO₂ present. The results are shown in Figures 3a-3d for 16 selected records, the details of which are given in Table 1. In this analysis the ozone distribution parameters, chosen to best fit the data, are W = 0.218, y_p = 25.0, and h = 4.53. In comparison with equation (1A) one can see that the only change is in y_p. This distribution is shown in Fig. 2. The line positions and intensities were taken from the recent tables of Clough and Kniezys.¹¹ Their data were used with T = 233°K and Δv = 2.5 cm⁻¹. The half-widths were derived from Walshaw's⁹ work and taken as γ⁰ = 0.085 cm⁻¹ atm⁻¹ at 233°K for all lines.

Most of the fine structure seen in the theoretical calculations in Fig. 3 is not a real spectral structure; it is due to the sharp edge of the square slit function.³ In the regions where the experimental curve is dashed, spurious absorptions occurred which are due to momentary sun-seeker lapse of control, as, for example, in the region 1025-1030 cm⁻¹ on record 29. In addition, all the records show a transmittance loss around 1000 cm⁻¹ the source of which is in doubt; it is either solar absorption or instrumental loss or both. This loss prevented the use of the end of the P-branch in determining the envelope.

It should be noted here that the resulted transmittance is quite insensitive to small changes in the values of these three parameters. For example, change of ~10% in the parameter h yields ~3% change in transmittance for records taken at 20-30 km altitude, and ~6% for records taken at 10-15 km altitude. The transmittance is similarly insensitive to changes in W or y_p.

From Fig. 3 it is seen that differences in transmittance between two consecutive experimental records are much greater than the corresponding differences in the calculated spectra. This effect, which is at many frequencies more than 5% difference is the main restriction in fitting the theoretical spectra to the experimental data. For example, the two consecutive records 19 and 20, which were taken at an altitude difference of ~1 km (compare Table 1) show significant differences of this kind at 1040 cm⁻¹ and around 1060 cm⁻¹. A similar kind of disagreement occurs in which the theoretical spectra fits the data well in one or two branches only but not in the remaining branches, while at the same time the agreement is close in neighboring records for all

three branches. For example, there is close agreement in the P-, Q- and R-branches in record 61, while in record 66 taken at only 1 km lower there is a nice agreement in the Q- and R-branches with a loss of agreement in the P-branch.

It is important to show that the previously noted differences between the theoretical spectra and the experimental data are not due to the approximations involved in using the statistical model combined with the CG approximation. For this purpose three records were selected for comparison between the different methods of calculation: one corresponds to ground measurements, record 9, one to record 20 and one to record 61. The altitudes and $\sec\theta$ for these three records are given

in Table 2. The calculated values p_E , L_E and $\int_{y_0}^{\infty} \rho(y)dy$ are also given

in the same Table. It is seen that while p_E changes from 0.037 to 0.096 atm, L_E changes from 9.4 to 9.9 cm; these variations are not enough for constructing curves of growth mentioned in Section 2.

The comparisons of transmittance calculations for the above records using the different methods are shown in Figs. 4-6. In each of these the two upper curves are displaced by 20% for convenience of comparison. It is seen that the agreement becomes closer with higher altitudes, but is still satisfactory for the low altitude record. The statistical model (curves 3 in Figs. 4-6) predicts somewhat more absorption than the exact line by line calculation (curves 1) and is very close to the CG approximation combined with line by line calculations (curves 2). The differences in transmittance are the largest around 1030 cm^{-1} and around 1060 cm^{-1} , where the exact calculation forms slight dips while the statistical model transmittance is smoothed out. However, the experimental data do not consistently reveal these dips clearly, as can be seen from Fig. 3, from records such as 19 and 20 around 1060 cm^{-1} .

The integrated absorptions over the band, $\int_{995.9}^{1068.7} A_v dv$, for the

above three records are compared in Table 3. It is seen that for the high altitude record the difference between the exact line by line calculation and the statistical model calculation is less than 3% while for the low altitude record this difference is less than 6%. Thus all the three

methods of calculation agree well and the agreement between either one of them with the data is much less than the agreement between themselves.

4. CONCLUSIONS

It is evident from the present analysis that for many frequencies with the band the increment in absorption between two consecutive line by line calculations and the corresponding increment calculated by the statistical model agree more closely than either agree with the increment observed in the reduced data. In view of this any decision as to which theoretical approach gives the best agreement with the experimental data will have to be delayed until better experimental data are available. The major problem with refining the experimental data is the determination of the correct envelope (which is a combination of the vacuum envelope and the instrumental response) in reference to which the transmittance is calculated. Since a better envelope is not presently available, it is not possible at this time to state to within what limits the various theoretical calculations will agree with the data. Certain use of the statistical based model combined with the Curtis-Godson approximation will give theoretical results in agreement with the experimental results to within the accuracy achieved in the experimental data presented here. This provides a simple way to analyze the atmospheric absorption in the 9.6μ ozone band. It is expected that this method would yield results in good agreement with experimental results as long as the resolution is not significantly better than 1.5 cm^{-1} .

It is realized that the real density distribution of ozone is highly variable, especially below 25 km, so that the distribution used here may deviate from the actual distribution at the time of the balloon flight. Since the theoretical results seem adequate this does not appear to limit the usefulness of the method.

ACKNOWLEDGMENTS

The line by line calculations were made using the programs devised by T. G. Kyle. These programs can produce efficiently theoretical spectra of gases for which the line parameters are known for any assumed line shape.

The computer time required for these programs and for other programs concerning the data reduction and the statistical band model calculations was made available by the National Center for Atmospheric Research, Boulder, Colorado.

The launch and recovery of the balloon instrumentation was capably handled by the Air Force Cambridge Research Laboratories Balloon R&D Test Group at Holloman Air Force Base, New Mexico.

REFERENCES

1. D. G. Murcray, F. H. Murcray and W. J. Williams, *Appl. Opt.* 6, 191 (1967).
2. M. Migeotte, L. Neven and J. Swensson, *The Solar Spectrum from 2.8 to 23.7 Microns; Part II. Measures and Identifications* Mem. Soc. Roy. Sci. Liege, Spec. Vol. No. 2 (1957).
3. A. Goldman and T. G. Kyle (to be published in *Appl. Opt.*).
4. C. D. Rodgers and C. D. Walshaw, *Quart. J. Roy. Meteor. Soc.* 92, 67 (1966).
5. D. J. McCaa and J. H. Shaw, "The Infrared Absorption Bands of Ozone," Contract AF 19(628)-3806, Scientific Report No. 2, Ohio State University, February 1967.
6. A. E. S. Green, *Appl. Opt.* 3, 203 (1964).
7. T. L. Altshuler, Fig. 18, Document No. 61SD199, December 1961, General Electric, M. S. V. D., Philadelphia, Pa.
8. U. S. Standard Atmosphere, 1962, U. S. Government Printing Office, Washington, D. C. (1962).
9. C. D. Walshaw, "An Experimental Investigation of the 9.6μ Band of Ozone," Ph. D. Thesis, Cambridge University, 1954.
10. A. Goldman and U. P. Oppenheim, *J. Opt. Soc. Am.* 55, 794 (1965).
11. S. A. Clough and F. X. Kneizys, "Ozone Absorption in the 9.0 Micron Region," Scientific Report AFCRL-65-862, 1965.
12. M. Griggs, "Atmospheric Ozone," Chapt. 4, pp. 83-118, in The Middle Ultraviolet: Its Science and Technology, edited by A. E. S. Green, (John Wiley, 1966).

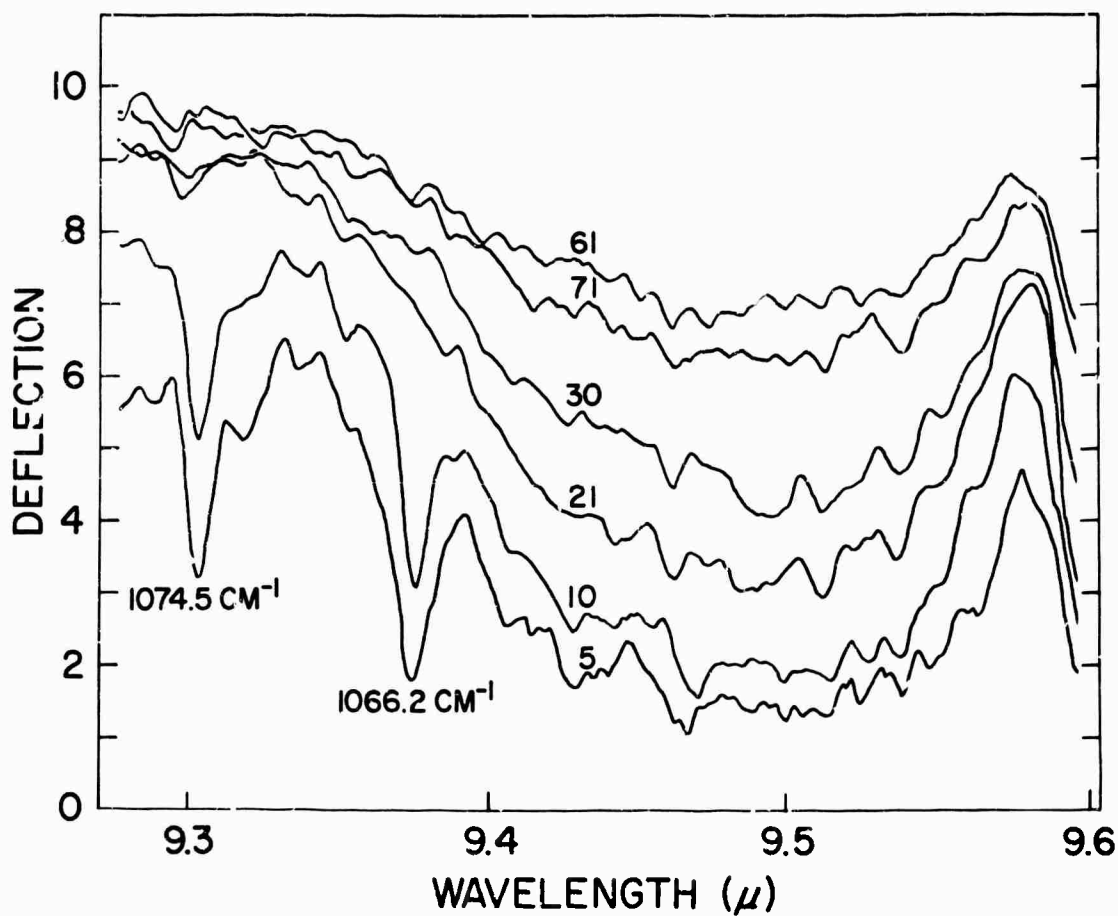


Figure 1. Samples of the unreduced data showing the variation of the R-branch of the $9.6\mu \text{O}_3$ band with altitude. Each is labelled by record number (5 to 61) for which details are given in Table 1.

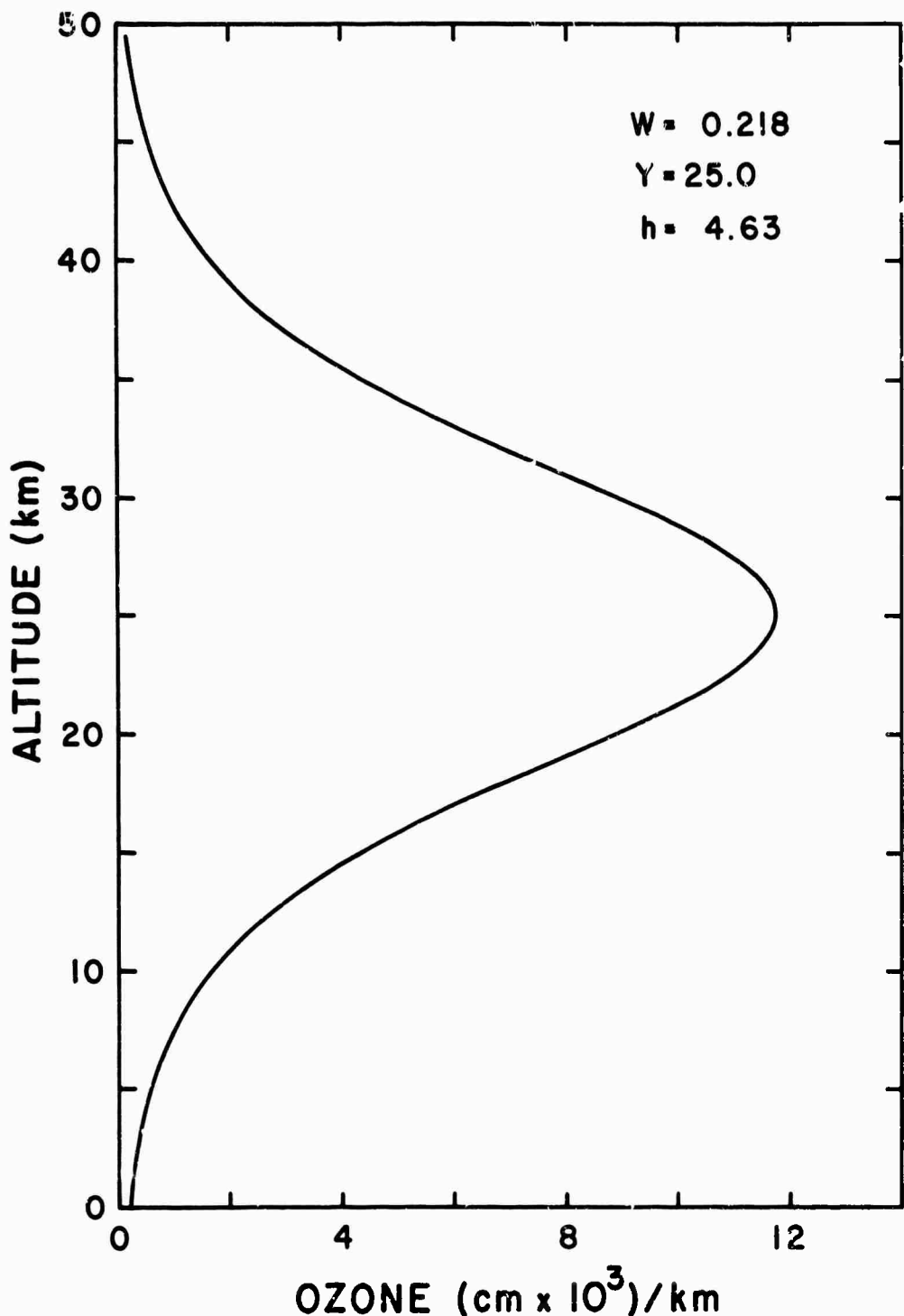


Figure 2. The selected analytical density distribution used here for ozone, with the parameters $W = 0.218$ cm-atm, $y_n = 25.0$ km and $h = 4.63$ km.

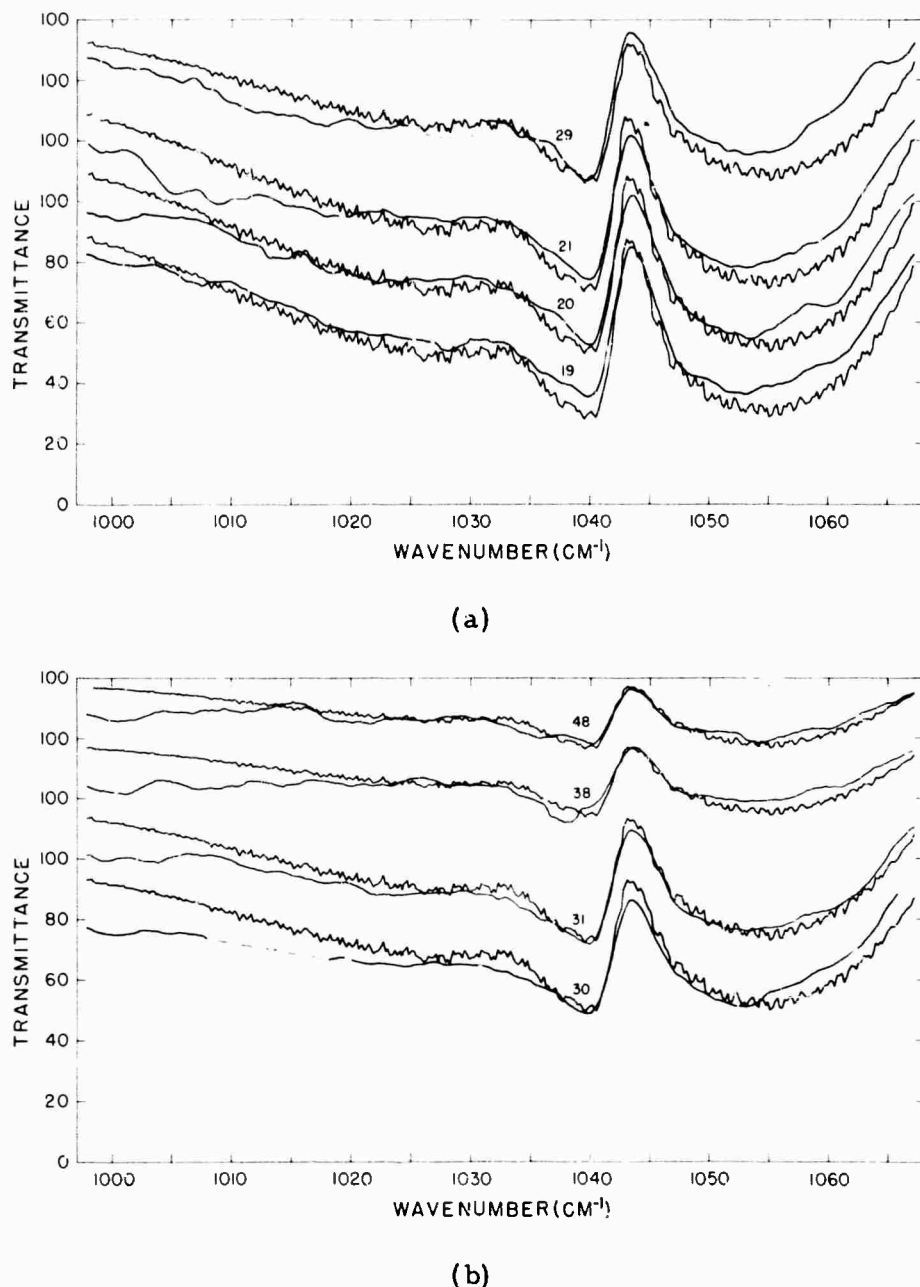


Figure 3. Comparison of observed and calculated transmittance by the $9.6\mu\text{O}_3$ band. The calculations were made using the statistical model combined with Curtis-Godson approximation with no water vapor present. The spectra are labelled according to record numbers, the details of each record number being given in Table 1. The relatively smooth curve is that of the reduced data while the wiggly curve is the theoretical curve.

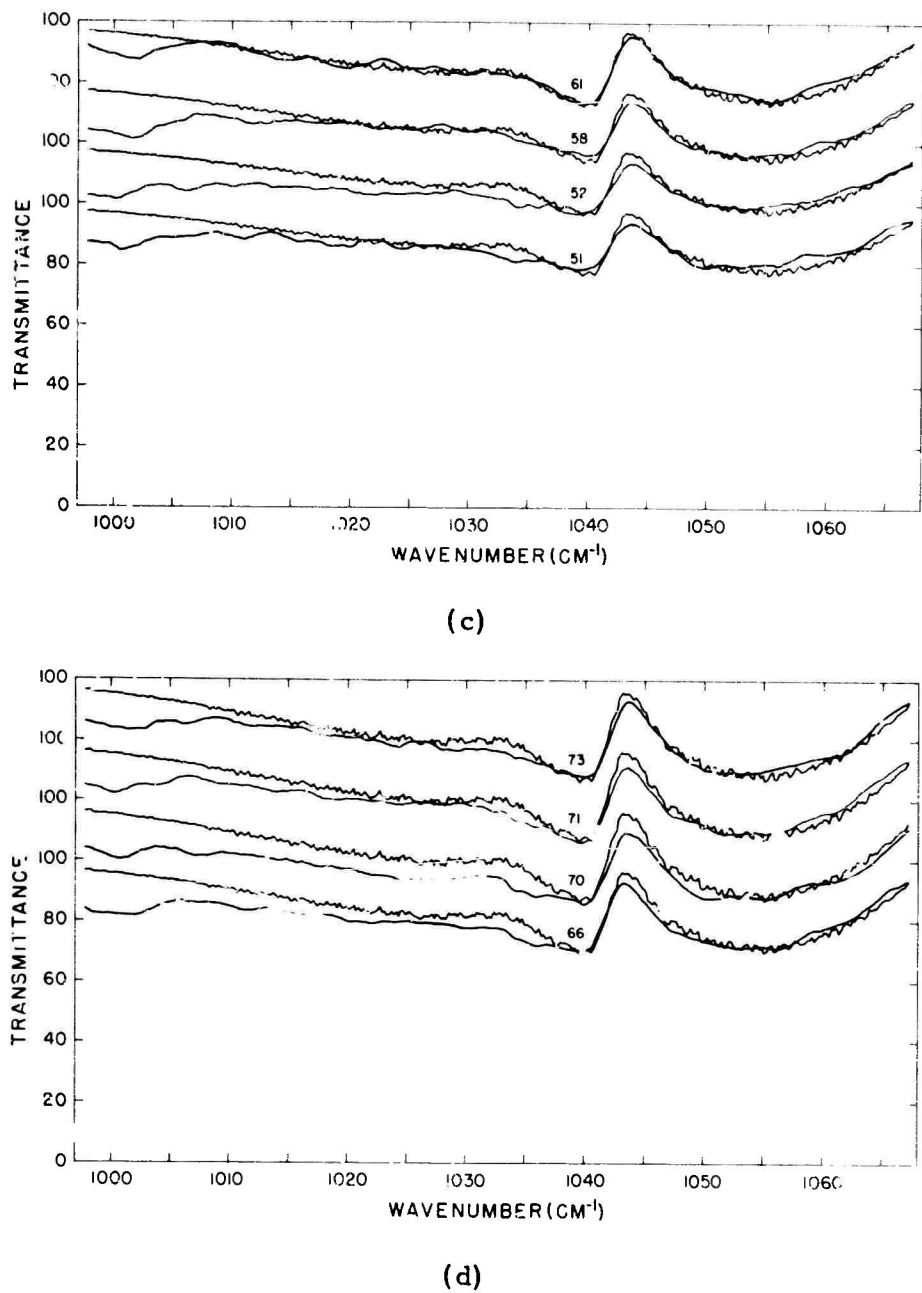


Figure 3. (Cont.)

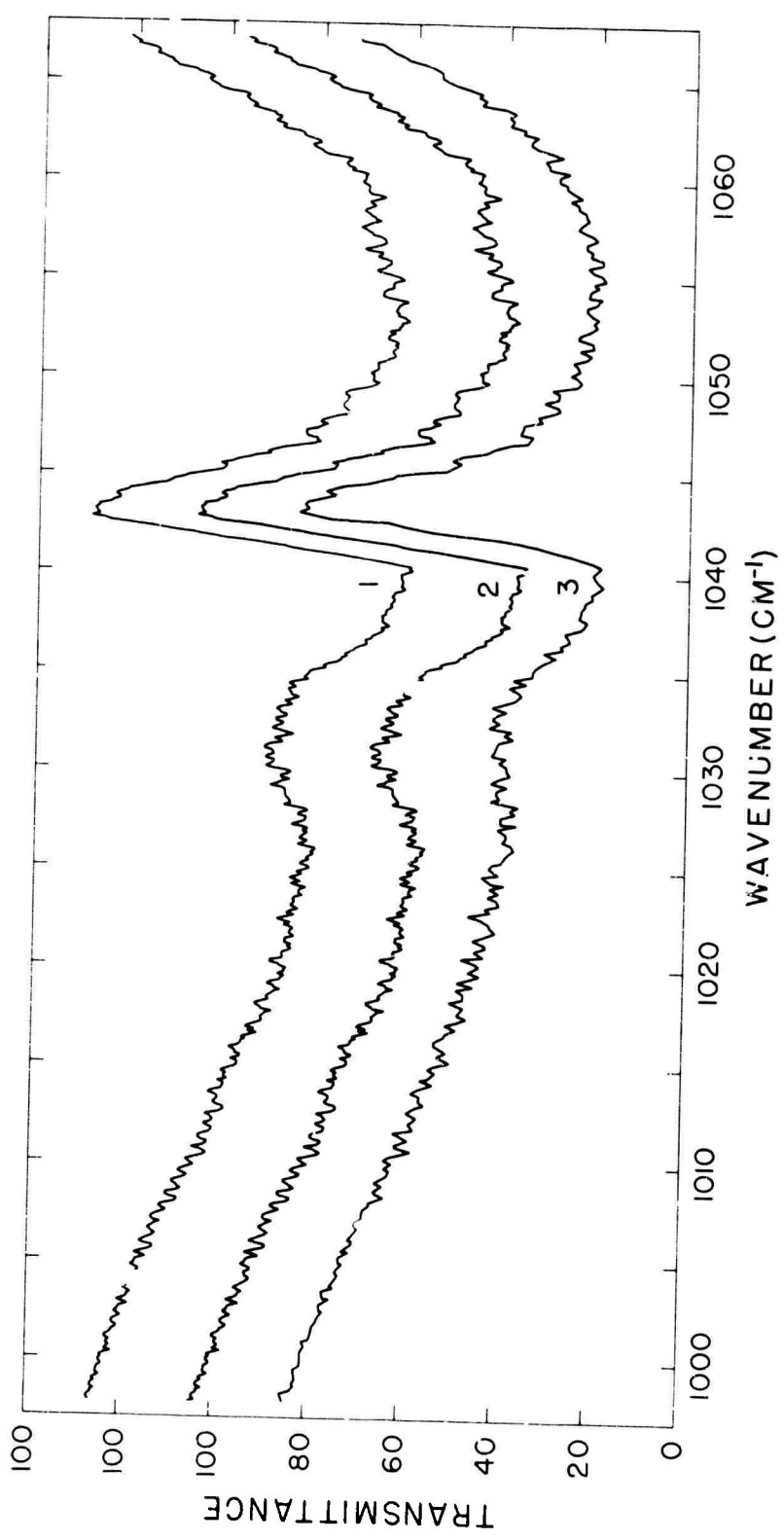


Figure 4. Comparison of transmittance obtained by exact line by line calculation, curve (1); by the combination of Curtis-Godson approximation and line by line calculation, curve (2); and by the combination of Curtis-Godson approximation and the statistical model curve (3); for the $9.6\mu\text{O}_3$ band. All the curves are calculated for Rec. 9 using the ozone distribution described in Fig. 2. Details for Record 9 are given in Table 1. The two upper curves are displaced by 20%.

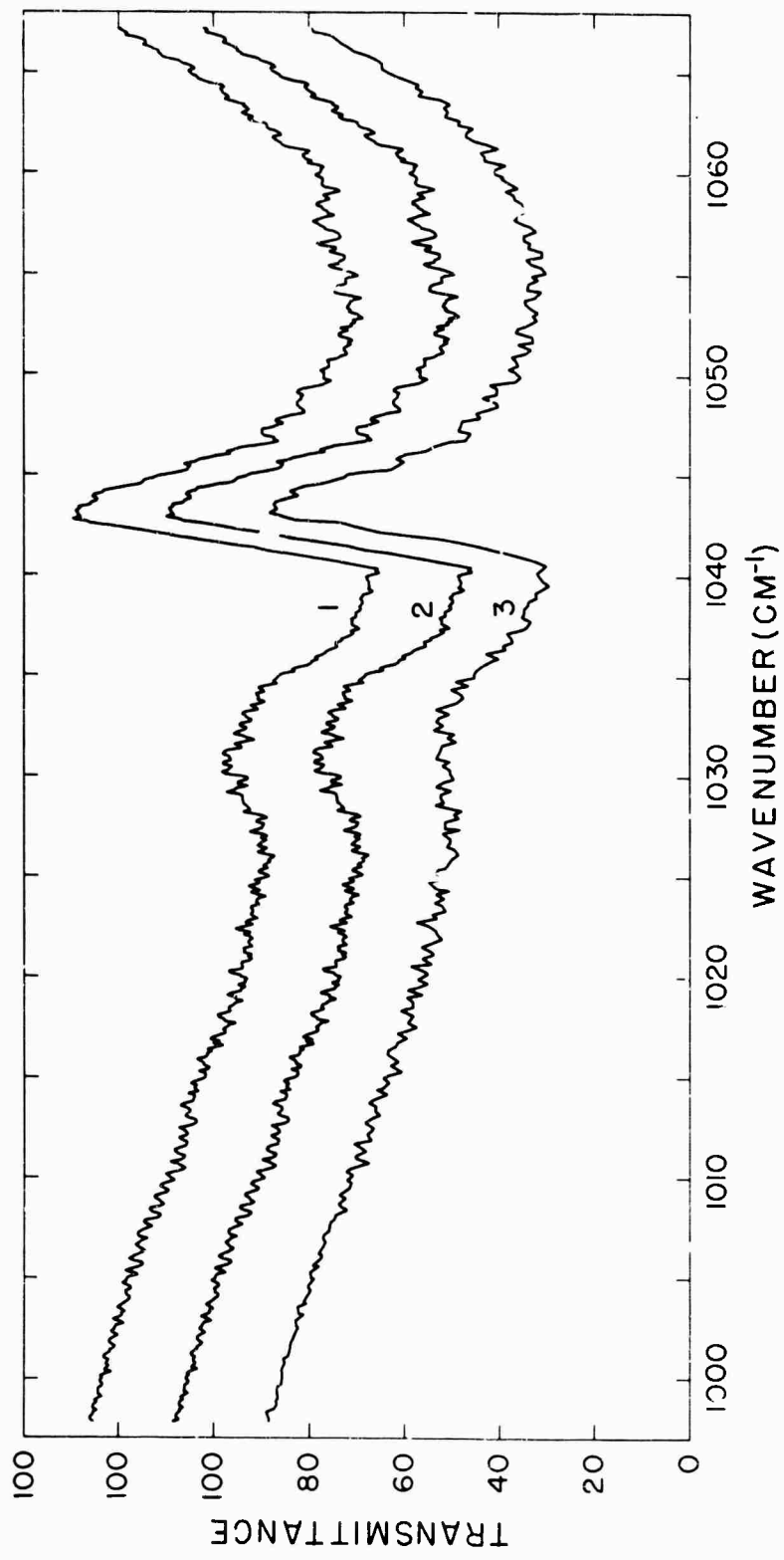


Figure 5. Comparison of transmittance obtained by exact line by line calculation, curve (1); by the combination of Curtis-Godson approximation and line by line calculation, curve (2); and by the combination of Curtis-Godson approximation and the statistical model, curve (3); for the $9.6\mu\text{O}_3$ band. All the curves are calculated for Rec 20 using the ozone distribution described in Fig. 2. Details for Rec. 20 are given in Table 1. The two upper curves are displaced by 20%.

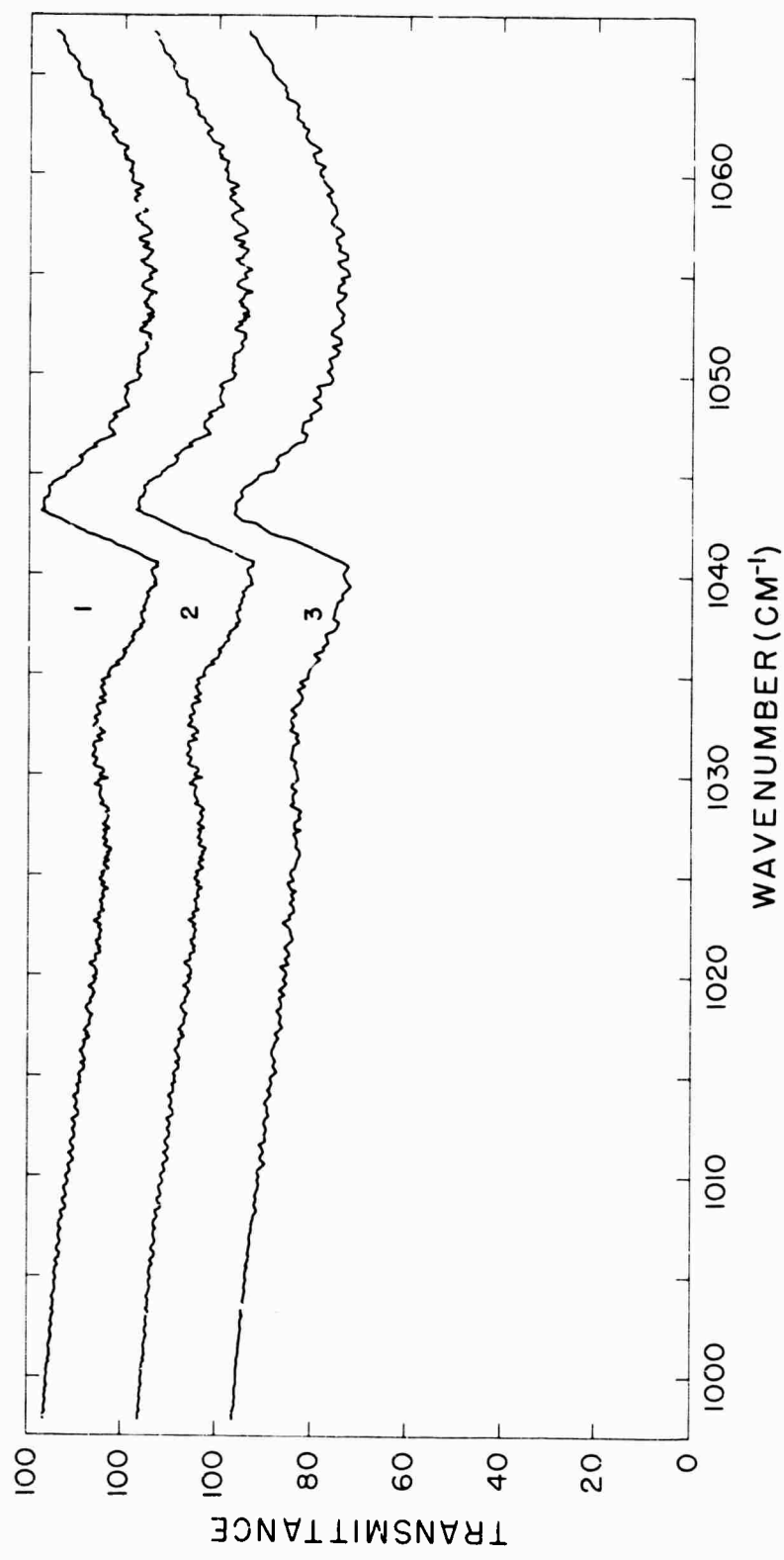


Figure 6. Comparison of transmittance obtained by exact line by line calculation, curve (1); by the combination of Curtis-Godson approximation and line by line calculation, curve (2); and by the combination of Curtis-Godson approximation and the statistical model, curve (3); for the $9.6\mu\text{m O}_3$ band. All the curves are calculated for Rec. 61 using the ozone distribution described in Fig. 2. Details for Rec. 61 are given in Table 1. The two upper curves are displaced by 20%.

TABLE 1

Times, altitudes, pressures and sec θ factors for selected records; the last 16 records were analyzed by the statistical model combined with Curtis-Godson approximation (see Fig. 3).

<u>Rec</u>	<u>Time(MST)</u>	<u>Altitude(km)</u>	<u>p(mb)</u>	<u>Sec θ</u>
5	7:54	1.25	872	2.38
10	8:07	2.71	727	2.17
19	8:46	10.79	235	1.74
20	8:50	11.83	200	1.71
21	8:54	12.95	167	1.68
29	9:28	20.02	55.5	1.48
30	9:33	21.21	46.0	1.46
31	9:37	22.25	39.0	1.44
38	10:07	28.60	14.7	1.33
48	10:50	29.40	13.0	1.23
51	11:03	29.20	13.3	1.21
52	11:07	29.20	13.3	1.21
58	11:33	28.30	15.3	1.18
61	11:45	27.50	17.3	1.18
66	12:07	26.50	20.1	1.18
70	12:24	25.90	22.1	1.18
71	12:28	25.80	22.4	1.18
73	12:37	25.90	23.0	1.19

TABLE 2

Altitudes, sec θ factors, equivalent pressures, equivalent path lengths and amounts of ozone for the three records, selected for comparison of the three methods of calculation.

<u>Rec.</u>	<u>Altitude (km)</u>	<u>Sec θ</u>	<u>P_E (atm)</u>	<u>L_E (cm)</u>	$\int_{y_0}^{\infty} \rho(y) dy$ (cm-atm)
9	2.07	2.23	0.05125	9.419	0.2165
20	11.83	1.71	0.03715	9.483	0.2060
61	27.50	1.18	0.00957	9.894	0.0803

TABLE 3

Integrated absorption $\int_{995.9}^{1068.7} A_\nu dv$ in cm^{-1} obtained by the three methods of calculation for the three selected records.

	<u>Rec. 9</u>	<u>Rec. 20</u>	<u>Rec. 61</u>
Exact line by line	35.95	32.22	10.52
Curtis-Godson and line by line	38.34	31.12	10.30
Curtis-Godson and Statistical Model	38.02	31.02	10.22

Unclassified

Security Classification

DOCUMENT CONTROL DATA - R & D

(Security classification of title, body of abstract and indexing annotation must be entered when the overall report is classified)

1. ORIGINATING ACTIVITY (Corporate author) University of Denver Department of Physics Denver, Colorado 80210		2a. REPORT SECURITY CLASSIFICATION Unclassified
		2b. GROUP
3. REPORT TITLE Atmospheric Absorption of Solar Radiation by the 9.6 μ Ozone Band		
4. DESCRIPTIVE NOTES (Type of report and inclusive date) Scientific. Interim.		
5. AUTHOR(S) (First name, middle initial, last name) Aharon Goldman Frank Murcay David Murcay Walter Williams		
6. REPORT DATE October 1967	7a. TOTAL NO OF PAGES 26	7b. NO OF REFS 12
8a. CONTRACT OR GRANT NO AF 19(628)-5202 ARPA ORDER No. 363	9a. ORIGINATOR'S REPORT NUMBER(S) Scientific Report No. 6	
b. PROJECT NO. Project, Task, Work Unit Nos. 8662-01-01 DoD Element 6250301R	9b. OTHER REPORT NO(S) (Any other numbers that may be assigned this report) AFCRL-67-0572	
10. DISTRIBUTION STATEMENT 1 - Distribution of this document is unlimited. It may be released to the Clearing-house, Department of Commerce, for sale to the general public.		
11. SUPPLEMENTARY NOTES This research was sponsored by the Advanced Research Projects Agency	12. SPONSORING MILITARY ACTIVITY Air Force Cambridge Research Laboratories (CRC) L. G. Hanscom Field Bedford, Massachusetts 01730	
13. ABSTRACT The statistical band model, combined with the Curtis-Godson approximation is applied to the analysis of atmospheric slant path absorption of the 9.6 μ O ₃ band. The theoretical spectra are compared with experimental absorptions observed during a balloon flight during which spectra were obtained at altitudes up to 30 km. The results are shown to agree to within the accuracy of the data. The band model method of calculation is compared to exact line by line calculation and to the combination of the Curtis-Godson approximation and line by line calculation. A surprisingly close agreement is found between the different methods of calculation, confirming the success of the application of the band model method to the data.		

Unclassified

Security Classification

14 KEY WORDS	LINK A		LINK B		LINK C	
	ROLE	WT	ROLE	WT	ROLE	WT
Solar Spectrum						
Infrared Spectrum						
Telluric Transmittance						
Stratospheric Ozone						

Unclassified

Security Classification